Published in final edited form as:

*Cell Rep*. 2017 July 18; 20(3): 655–667. doi:10.1016/j.celrep.2017.06.080.

# Loss of hepatic mitochondrial long chain fatty acid oxidation confers resistance to diet-induced obesity and glucose intolerance

**Jieun Lee**[1,4], **Joseph Choi**[1,4], **Ebru S. Selen Alpergin**[1,4], **Liang Zhao**[5], **Thomas Hartung**[5,7], **Susanna Scafidi**[2], **Ryan C. Riddle**[3,6], and **Michael J. Wolfgang**[1,4,8,*]

[1]Department of Biological Chemistry, Johns Hopkins University School of Medicine, Baltimore, Maryland 21205 [2]Department of Anesthesiology and Critical Care Medicine, Johns Hopkins University School of Medicine, Baltimore, Maryland 21205 [3]Department of Orthopadedic Surgery, Johns Hopkins University School of Medicine, Baltimore, Maryland 21205 [4]Center for Metabolism and Obesity Research, Johns Hopkins University School of Medicine, Baltimore, Maryland 21205 [5]Department of Environmental Health and Engineering, Bloomberg School of Public Health, Johns Hopkins University, Baltimore, MD 21205, USA [6]Baltimore Veterans Administration Medical Center, Baltimore, Maryland [7]Department of Biology, University of Konstanz, 78464 Konstanz, Germany

## SUMMARY

The liver has a large capacity for mitochondrial fatty acid β-oxidation, which is critical for systemic metabolic adaptations such as gluconeogenesis and ketogenesis. To understand the role of hepatic fatty acid oxidation in response to a chronic high fat diet (HFD), we generated mice with a liver-specific deficiency of mitochondrial long chain fatty acid β-oxidation ($Cpt2^{L-/-}$ mice). Paradoxically, $Cpt2^{L-/-}$ mice were resistant to HFD-induced obesity and glucose intolerance with an absence of liver damage, although they exhibited serum dyslipidemia, hepatic oxidative stress and systemic carnitine deficiency. Feeding a HFD induced hepatokines in mice with a loss of hepatic fatty acid oxidation that enhanced systemic energy expenditure and suppressed adiposity. Additionally, the suppression in hepatic gluconeogenesis was sufficient to improve HFD-induced glucose intolerance. These data show that inhibiting hepatic fatty acid oxidation results in a systemic hormetic response that protects mice from HFD-induced obesity and glucose intolerance.

[*]Address correspondence to: Michael J. Wolfgang, Ph.D, Department of Biological Chemistry, Johns Hopkins University School of Medicine, 855 N. Wolfe St., 475 Rangos Building, Baltimore, MD 21205, Tel: 443-287-7680, mwolfga1@jhmi.edu.
[8]Lead contact

**Conflict of interest**

The authors declare that they have no conflicts of interest with the contents of this article.

**Author contributions**

J.L., J.C, E.S.A. and R.C.R. conducted the experiments and analyzed the results. E.S.A. conducted the NMR experiments and analyzed the results. E.S.A, L.Z. and T.H. conducted the isotopologue labeling experiment. M.J.W. conceived the idea for the project. J.L. J.C. and M.J.W. wrote the paper with input and approval of all authors.

## eTOC

Lee et al. show that contrary to expectations, the loss of hepatic fatty acid oxidation (FAO) confers resistance to weight gain and adiposity in response to a high fat diet. Additionally, they show that loss of heptic FAO, and consequently hepatic gluconeogenesis, protects mice from high fat diet-induced glucose intolerance.

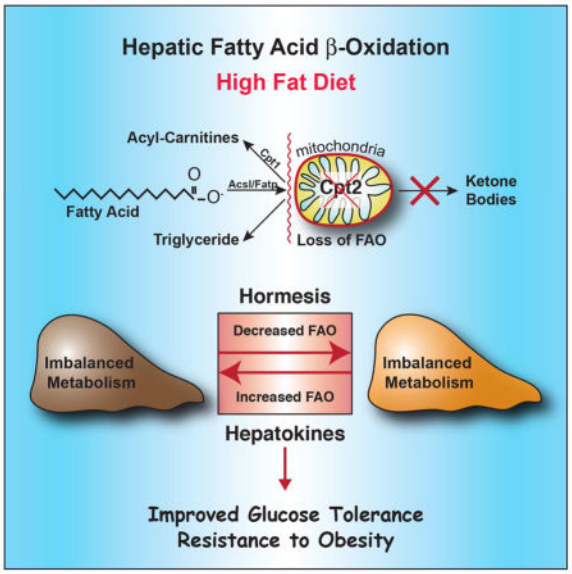


## INTRODUCTION

The metabolism, storage and flux of lipids in the liver plays a central role in diet-induced obesity, diabetes and nonalcoholic fatty liver disease (NAFLD). However, the detailed mechanisms governing the shift from normal physiology to pathophysiology are poorly understood, particularly with respect to the role of lipid metabolism. The liver represents a metabolic hub for the uptake and distribution of lipids via free fatty acids, lipoproteins and de novo lipogenesis. Consequently, an imbalance between hepatic lipid uptake/anabolism and export/catabolism in chronic states of over-nutrition has been implicated in the etiology of many obesity-related diseases. (Mashek, 2013; Samuel et al., 2004; Savage et al., 2007; Szendroedi et al., 2011). The liver has a large capacity for mitochondrial fatty acid β-oxidation and represents a major catabolic pathway in hepatocytes. Inborn errors in fatty acid oxidation often present with serious metabolic disease that center on hepatic function. Additionally, many chronic diseases exhibit disruptions in hepatic mitochondrial fatty acid oxidation (Samuel et al., 2004; Savage et al., 2007).

Long chain fatty acids are first activated in the cytosol to long chain acyl-CoAs via long chain acyl-CoA synthetases. In order to traverse the mitochondrial membrane and gain access to the mitochondrial matrix, long chain acyl-CoAs depend on carnitine and carnitine palmitoyltransferases. Activated long chain acyl-CoAs are converted to long chain acylcarnitines via carnitine palmitoyltransferase 1 (Cpt1) located on the mitochondrial outer membrane. Long chain acylcarnitines can then translocate into the mitochondrial matrix via

the carnitine:acylcarnitine translocase, where they are finally converted back to long chain acyl-CoAs via carnitine palmitoyltransferase 2 (Cpt2) (Kerner and Hoppel, 2000; McGarry and Brown, 1997). Cpt1 is encoded by multiple genes that exhibit differential tissue specificity (Kerner and Hoppel, 2000). However, Cpt2 is encoded by a single gene. Long chain acyl-CoAs generated by Cpt2 can then be processed through β-oxidation to provide the carbon substrate for ketogenesis (acetyl-CoA) and mitochondrial bioenergetics (ATP, NADH, $FADH_2$) to facilitate gluconeogenesis. (Chen et al., 1999; Kerner and Hoppel, 2000; McGarry and Brown, 1997; Soling et al., 1968). Previously, we generated a mouse model with a conditional loss-of-function of *Cpt2* specifically in the liver (referred to herein as $Cpt2^{L-/-}$ mice) that are deficient in hepatic mitochondrial long chain fatty acid β-oxidation. $Cpt2^{L-/-}$ mice were relatively normal under carbohydrate-fed conditions, but fasting resulted in hepatic steatosis and serum dyslipidemia with an absence of circulating ketone bodies. Feeding a ketogenic diet to $Cpt2^{L-/-}$ mice resulted in severe hepatomegaly, liver damage and death with a complete absence of adipose triglyceride stores (Lee et al., 2016b). As expected, hepatic fatty acid oxidation was a critical adaptation to fasting.

To understand the role of hepatic fatty acid β-oxidation in response to a chronic high fat diet (HFD), we challenged $Cpt2^{L-/-}$ and control mice to a long-term high fat feeding. Unexpectedly, $Cpt2^{L-/-}$ mice were resistant to HFD-induced obesity and glucose intolerance with an absence of liver damage, although they exhibited serum dyslipidemia, hepatic oxidative stress and systemic carnitine deficiency. The suppression in adiposity and obesity was associated with a HFD-dependent increase in whole body energy expenditure that was normalized by lowering energy expenditure via thermoneutral housing. Additionally, the deficiency in fatty acid oxidation suppressed hepatic glucose production, resulting in greatly improved glucose tolerance. These data demonstrate the central role of hepatic fatty acid oxidation to systemic energy homeostasis and highlight a surprisingly beneficial role of inhibiting hepatic fatty acid oxidation to systemic metabolic dysfunction.

## RESULTS

### Mice with a loss of hepatic fatty acid oxidation are resistant to high fat diet-induced obesity

Previously, we showed that $Cpt2^{L-/-}$ mice were relatively normal under carbohydrate-fed conditions, but the exposure of the liver to a high burden of free fatty acids via prolonged fasting or a ketogenic diet elicited profound cellular and physiological adaptations (Lee et al., 2016b). Since hepatic fatty acid oxidation is central to systemic energy balance, we were interested in how feeding a chronic lipid-rich diet to $Cpt2^{L-/-}$ mice would affect systemic metabolic dysfunction. Therefore, we placed $Cpt2^{L-/-}$ and littermate control ($Cpt2^{lox/lox}$) mice on a high fat (HFD) or low fat diet (LFD) for 16 weeks. Although $Cpt2^{L-/-}$ mice have a genetically imposed deficiency in energy expenditure, both male and female $Cpt2^{L-/-}$ mice were paradoxically resistant to HFD-induced body weight gain. (Figures 1A, 1A′). The loss of hepatic fatty acid oxidation did not affect body size as there was no genotypic change in femur length. The suppression in body weight in HFD-fed $Cpt2^{L-/-}$ mice was due largely to a reduction of fat mass (Figures 1B, 1B′). $Cpt2^{L-/-}$ mice fed a LFD for 16 weeks did not exhibit changes in body weight, although both male and female mice had a small

suppression in fat mass (Figure S1). The suppression in fat mass in male mice was mainly due to a decrease in iWAT (Figure 1C). Histological examination of iWAT demonstrated smaller adipocytes in HFD-fed $Cpt2^{L-/-}$ mice compared to control mice (Figures 1D, 1E). These data show that a loss of hepatic fatty acid oxidation paradoxically results in resistance to HFD-induced obesity and adiposity.

To further understand the systemic response to a loss of hepatic fatty acid oxidation under HFD-fed conditions, we examined circulating metabolites in $Cpt2^{lox/lox}$ and $Cpt2^{L-/-}$ mice. As expected, $Cpt2^{L-/-}$ mice exhibited suppressed β-hydroxybutyrate and increased NEFA (Figure 1F). Additionally, $Cpt2^{L-/-}$ mice had greatly improved glucose and insulin levels more indicative of LFD-fed mice (Figure 1G). Consistent with decreased adiposity and improved glucose homeostasis, leptin was lower and adiponectin was unchanged in $Cpt2^{L-/-}$ mice. (Figure 1H). Previously, we had shown significant alterations in serum acylcarnitines in $Cpt2^{L-/-}$ mice in response to a 24hr fast or feeding a ketogenic diet (Lee et al., 2016b). HFD-fed $Cpt2^{L-/-}$ mice exhibited a dramatic suppression of free carnitine and acetyl-carnitine in both blood (Figure 1I) and urine (Figure 1J). Other short chain fatty acids were also significantly lower in HFD-fed $Cpt2^{L-/-}$ mice. Interestingly, $Cpt2^{L-/-}$ mice exhibited more medium chain monounsaturated acylcarnitines in their urine, suggesting a cell nonautonomous effect on the kidney (Figure 1J). These data show that the loss of hepatic fatty acid oxidation alters systemic lipid metabolism and improves glucose homeostasis following chronic high fat feeding.

## High fat diet elicits oxidative stress and a hormetic response in $Cpt2^{L-/-}$ mice

The loss of hepatic fatty acid oxidation would be predicted to potentiate HFD-induced hepatic steatosis. Surprisingly, 16wks of HFD feeding did not exacerbate hepatic steatosis or liver triglyceride (TAG) content in $Cpt2^{L-/-}$ livers (Figures 2A, 2B). Interestingly, although $Cpt2^{L-/-}$ livers did not exhibit potentiated steatosis, there was a loss of metabolic zonation evident in control livers (Figure 2A). A potential explanation for the resistance to weight gain in $Cpt2^{L-/-}$ mice could be liver failure. However, other than reduced adiposity, $Cpt2^{L-/-}$ mice were overtly indistinguishable from littermate controls. Additionally, there was no difference in serum ALT activity, a measure of liver damage (Figure 2C). These data show that the loss of hepatic fatty acid oxidation does not result in potentiated fatty liver or liver damage following chronic high fat feeding.

Defects in mitochondrial oxidative metabolism can increase oxidative stress. Therefore, we determined markers of oxidative stress in $Cpt2^{L-/-}$ and control HFD-fed mice. The livers of $Cpt2^{L-/-}$ mice exhibited increased lipid peroxidation and decreased glutathione content indicative of increased oxidative burden (Figures 2D, 2E). Serum lipid peroxidation was not affected (Figure S2A). Consistent with an increase in oxidative stress, the Hsp27 protein, which is induced upon oxidative stress, was increased in $Cpt2^{L-/-}$ livers (Figure 2F). Next, we profiled genes involved in oxidative stress via PCR array. Although there were few significant transcriptional changes in genes that are involved in the oxidative stress pathway, we observed a substantial reduction in *Scd1* expression (Figure S2B). In a larger cohort, we examined the expression of other genes in fatty acid biosynthesis. $Cpt2^{L-/-}$ livers showed a significant suppression of fatty acid biosynthetic genes *Acly, Acc, Fasn, Srebp1* and *Scd1*

(Figure 2G). These changes were confirmed at the protein level for Acly, Acc, Fasn, and Scd1 (Figure 2H). Additionally, we assayed the expression of peroxisomal and autophagy related genes (Lee et al., 2014; Zhang et al., 2007). We observed small transcriptional changes in *Cyp4a1*, *Lc3b* and *Gabarap1* (Figure S2C). To further understand the impact of a deficiency of fatty acid oxidation on fatty acid metabolism, we analyzed the fatty acid composition of $Cpt2^{L-/-}$ liver and iWAT. $Cpt2^{L-/-}$ liver exhibited a small increase in total fatty acids (Figure 2I, Table S2). Interestingly, the liver was enriched in medium chain fatty acids and depleted in C20–C22 length fatty acids (Figure 2J). Although we have not observed changes in very long chain fatty acid oxidation (C24:0) in $Cpt2^{L-/-}$ livers (Lee et al., 2016b), these data suggest that in the absence of mitochondrial oxidation, long chain fatty acid chain shortening in the peroxisome can be accelerated.

Although $Cpt2^{L-/-}$ livers exhibited increased oxidative stress and suppressed biosynthetic genes following chronic high fat feeding, the expression of mitochondrial proteins was not changed between $Cpt2^{L-/-}$ and $Cpt2^{lox/lox}$ mice (Figure 3A). On the other hand, genes involved in fatty acid oxidation, such as *Acot1, Acot2, Acox1, Cpt1a, Acadm, Acadl,* and *Hadha*, as well as canonical Pparα target genes *Pdk4* and *Ehhadh* and stress-induced genes such as *Atf3* were increased in $Cpt2^{L-/-}$ livers (Figure 3B) albeit to a lesser degree than fasting or a ketogenic diet (Lee et al., 2016b). In addition to the fatty acid oxidative genes being upregulated, there was an increase in mRNA expression of the hepatokines *Igfbp1*, *Gdf15* and *Fgf21* (Figure 3C). This was reflected in an increase in serum levels of Igfbp1, Gdf15 and Fgf21, suggesting that these hepatokines are contributing to physiological adaptations in response to a loss of mitochondrial fatty acid oxidation (Figure 3D). Due to the reported role of Igfbp1 and Fgf21 in bone we measured aspects of bone quality (Wang et al., 2015). The increase in these hepatokines did not affect long bone growth (Figure 1A, 1B) or bone structure (Figure S3). These data suggest that in response to the high lipid burden from a HFD, the liver is not only attempting to compensate for the loss of fatty acid oxidation by up-regulating oxidative programming, but also seeking to increase catabolism in peripheral tissues by way of secreted hepatokines. These data are consistent with a beneficial hormetic response.

## Loss of fatty acid oxidation suppresses hepatic gluconeogenesis

To probe further into the role of hepatic fatty acid oxidation in the metabolic alterations elicited by chronic high fat feeding, we performed $^{1}$H-NMR based steady-state metabolomics analysis on serum, liver and kidney of $Cpt2^{L-/-}$ and $Cpt2^{lox/lox}$ mice fed a HFD for 16wks. Consistent with the putative requirement of fatty acid oxidation on gluconeogenesis, the liver exhibited a >6-fold suppression in glucose as well as a suppression in many gluconeogenic substrates such as lactate, alanine and glutamine (Figure 4A). Consistent with an improvement in blood glucose, $Cpt2^{L-/-}$ serum showed a decrease in glucose and suppressed β-hydroxybutyrate (Figure 4B). These improvements were mirrored in the kidney metabolome (Figure 4C). These data suggest that the reduction in serum and hepatic glucose levels in $Cpt2^{L-/-}$ mice resulted from reduced hepatic gluconeogenesis. To investigate directly whether the loss of Cpt2 inhibited hepatic gluconeogenesis as expected by the steady-state data as well as its putative role, we traced the incorporation of 1-$^{13}$C-lactate into glucose in 24hr fasted $Cpt2^{L-/-}$ and $Cpt2^{lox/lox}$ mice

by a combination of NMR and mass spectrometry. 1-$^{13}$C-Lactate carbon enrichment was observed in the third (C3) and fourth (C4) position of glucose as previously described (Wolfe, 1992). Comparison of $^{13}$C-Glucose chemical shifts with BMRB $^{13}$C glucose reference showed expected C enrichments in C3 and C4 of glucose and incorporation at C3 and C4 were lower in Cpt2$^{L-/-}$ mice compared to Cpt2$^{lox/lox}$ mice (Figure 4D). To further validate the NMR results, we profiled 1-$^{13}$C-lactate-derived isotopologues of glucose (from m+0 to m+2) using HPLC/QTOF (Figure 4E). MS analysis of stable isotope distribution supported the NMR results; total glucose and the percentages of 1-$^{13}$C-lactate derived carbons in glucose isotopologues were significantly lower in Cpt2$^{L-/-}$ mice. These data confirm the putative requirement for fatty acid oxidation on the *de novo* production of glucose in the liver.

## Cpt2$^{L-/-}$ mice exhibit altered bile acid metabolism

One of the most surprising results from the metabolomics analysis was that glycine was significantly reduced in the livers of Cpt2$^{L-/-}$ mice measured via $^{1}$H-NMR (Figure 4A); however, serum and kidney glycine were significantly elevated (Figure 4B, 4C). Glycine is often referred to as a conditionally essential amino acid. That is, *de novo* production cannot keep up with demand because it is at the crossroads of many pathways. One potential sink for hepatic glycine is glutathione, which is indeed suppressed in HFD-fed Cpt2$^{L-/-}$ livers (Figure 2E). Another potential sink is in the production of bile acids and consistent with this notion, there was an increase in serum bile acids in HFD-fed Cpt2$^{L-/-}$ mice compared to Cpt2$^{lox/lox}$ mice (Figure 4F). Because of the increase in total bile acids, we examined bile acid metabolic genes in the liver and ileum to determine if the loss of fatty acid oxidation altered the transcriptional programming of bile acid metabolism. There were no significant changes in genes involved in bile acid metabolism in the livers of Cpt2$^{L-/-}$ and Cpt2$^{lox/lox}$ mice (Figure S4). Fgf15, a bile acid responsive gene derived from the ileum, has been shown to positively affect whole body energy expenditure (Potthoff et al., 2012). However, *Fgf15* was suppressed in the ileum of Cpt2$^{L-/-}$ mice as well as other bile acid responsive genes such as *ibabp* (Figure 4G). These data suggest that while bile acid metabolism is altered in Cpt2$^{L-/-}$ mice, Fgf15 is likely not responsible for the resistance to HFD-induced obesity in this model.

## Cpt2$^{L-/-}$ mice exhibit improved glucose tolerance and insulin sensitivity

Previously we have shown that Cpt2$^{L-/-}$ mice are able to maintain euglycemia during a 24hr fast (Lee et al., 2016b). Here we have shown that fatty acid oxidation is required for hepatic gluconeogenesis, and mice fed a HFD for 16wks exhibit marked improvements in glucose and insulin. To understand the role of hepatic fatty acid oxidation on systemic glucose metabolism, we first performed ipGTT on chow-fed 9wk old mice. Cpt2$^{L-/-}$ mice cleared blood glucose modestly more efficiently than Cpt2$^{lox/lox}$ mice during the ipGTT, suggesting that the mice were more insulin sensitive (Figure 5A). To further determine the role of hepatic fatty acid oxidation on gluconeogenesis and insulin sensitivity, we performed hyperinsulinemic-euglycemic clamp studies on Cpt2$^{L-/-}$ and control mice. As expected, these studies showed impaired endogenous glucose production during the hyperinsulinemic-euglycemic clamp (Figure 5B). These data demonstrate an increased ability of insulin to suppress endogenous glucose production in these mice (Figure 5B). However, insulin-

stimulated glucose uptake in skeletal muscle and adipose were not affected (Figure S5). These data are consistent with the idea that inhibiting hepatic fatty acid oxidation and therefore hepatic gluconeogenesis may be sufficient to improve systemic glucose handling.

Feeding a HFD to $Cpt2^{L-/-}$ mice for 16wks resulted in substantial improvements in glucose and insulin. However, the suppression in adiposity in $Cpt2^{L-/-}$ mice represents a significant confounder in those experiments. Therefore, we fed a new cohort of mice a HFD for 4wks, which is sufficient to generate glucose intolerance but before apparent changes in body weight or composition (Figures 1A, 1B, 4C). $Cpt2^{L-/-}$ mice exhibited an improvement in ipGTT compared to control mice fed a HFD for 4wks (Figure 5D). Also, basal and glucose-induced serum insulin was markedly improved in $Cpt2^{L-/-}$ mice (Figure 5E). Finally, $Cpt2^{L-/-}$ mice exhibited improved ipITT following the short-term HFD challenge (Figure 5F). Together these data support the idea that suppressed hepatic glucose production is sufficient to improve systemic glucose dysfunction.

## The loss of hepatic fatty acid oxidation enhances whole body energy expenditure in response to high fat feeding

Decreased body weight, adiposity and increased systemic catabolism upon a HFD in $Cpt2^{L-/-}$ mice led us to determine whole body bioenergetics in $Cpt2^{lox/lox}$ and $Cpt2^{L-/-}$ mice. In our previous studies, we found no differences in metabolic parameters between 9wk-old $Cpt2^{lox/lox}$ and $Cpt2^{L-/-}$ mice fed a chow diet, even following a 24hr fast (Lee et al., 2016b). Again, because altered body weight and adiposity are major confounders to energy expenditure, we fed $Cpt2^{lox/lox}$ and $Cpt2^{L-/-}$ mice a HFD for 4wks before significant changes in body weight were observed. $Cpt2^{L-/-}$ mice exhibited an increase in energy expenditure in both the light and dark phases (Figure 6A, 6B). To determine if a loss of hepatic fatty acid oxidation resulted in increased brown or beige fat, we measured thermogenic genes in interscapular brown adipose tissue (iBAT) and inguinal white adipose tissue (iWAT). $Cpt2^{L-/-}$ iBAT showed no difference in the expression of these genes, and $Cpt2^{L-/-}$ iWAT exhibited a significant suppression of *Ucp1*, *Dio2* and *Fgf21* (Figure S6). These data suggest a brown/beige adipocyte-independent increase in energy expenditure. There was no change in body weight or lean mass, but $Cpt2^{L-/-}$ mice exhibited a small decrease in fat mass even at this time point (Figure 6B). Interestingly $Cpt2^{L-/-}$ mice also displayed a small increase in food intake; however, there was no change in the respiratory exchange ratio (Figure 6B), suggesting that between $Cpt2^{lox/lox}$ and $Cpt2^{L-/-}$ mice, there was no preference in whole body fatty acid or glucose utilization in a genotype-specific manner. These data suggest the increased energy expenditure could be driving the resistance to HFD-induced obesity seen in $Cpt2^{L-/-}$ mice.

## Thermoneutral housing normalizes body weight gain and adiposity in $Cpt2^{L-/-}$ mice

We next sought to determine the contribution of the HFD-induced increase in energy expenditure in $Cpt2^{L-/-}$ mice to body weight gain and adiposity. Standard housing conditions (21°C) impose a mild cold stress to mice, thereby increasing their energy expenditure as well as food intake (Lee et al., 2016a). In order to suppress energy expenditure, we housed $Cpt2^{lox/lox}$ and $Cpt2^{L-/-}$ female mice in a thermoneutral environment (30°C) and fed a HFD for 16wks. Under standard housing conditions, $Cpt2^{L-/-}$

mice exhibited resistance to HFD-induced obesity (Figure 1A, 1A′); however, housing mice at a thermoneutral environment eliminated this difference (Figure 7A). Under standard housing conditions, female Cpt2$^{L-/-}$ mice exhibited a suppression in both iWAT and gWAT. The size of both of these depots were normalized at thermoneutrality while the increase in liver weight of Cpt2$^{L-/-}$ mice was not affected by ambient temperature (Figure 7B). Hepatic triglycerides and insulin were not changed between groups (Figure S7). Finally, we examined the effect of thermoneutrality on the hepatic genes that we have shown to be affected by a loss of Cpt2. There was an amelioration of hepatic *Igfbp1* expression by thermoneutral housing, but *Atf3*, *Gdf15* and *Fgf21* continued to be upregulated in Cpt2$^{L-/-}$ livers regardless of ambient temperature. Pparα target genes in the liver, such as *Pdk4*, *Acot1*, *Acot2* and *Ehhadh*, were suppressed by thermoneutral housing but were still increased in Cpt2$^{L-/-}$ livers compared to control (Figure 7C). These data suggest that the resistance to HFD-induced obesity in mice with a loss of hepatic fatty acid oxidation is mediated by an increase in systemic energy expenditure.

## DISCUSSION

The oxidation of long chain fatty acids in hepatocytes represents a major energetic pathway not only for the liver but also for the animal as a whole. Hepatic fatty acid oxidation is at the crossroads of important biological adaptations, particularly during times of increased lipid burden. Therefore, even small changes in hepatic fatty acid oxidation are often invoked as a mechanism to explain the phenotypes of models of obesity, diabetes and NAFLD. The appeal of this idea is that if a defect in hepatic fatty acid oxidation can exacerbate the metabolic syndrome then enhancing hepatic fatty acid oxidation could represent an effective therapy. In contrast to this rational extrapolation, mice with a hepatic-specific deficiency in mitochondrial fatty acid oxidation (Cpt2$^{L-/-}$ mice) are resistant to—instead of prone to—the major pathophysiologic features elicited by a HFD, including obesity and glucose intolerance, even though the mice have a genetically-imposed deficiency in hepatic energy expenditure.

The response of Cpt2$^{L-/-}$ mice to a HFD is similar to models of increased hepatic oxidative metabolism in general or fatty acid oxidation in particular (An et al., 2004; Orellana-Gavalda et al., 2011; Perry et al., 2013; Stefanovic-Racic et al., 2008). Although at face value these results are seemingly at odds, this biphasic response is most aptly defined as hormesis (Yun and Finkel, 2014). We have previously shown that Cpt2$^{L-/-}$ mice fasted for 24hr or fed a ketogenic diet enlist a host of adaptations in an attempt to maintain systemic energy homeostasis during these short-term challenges (Lee et al., 2016b). Here, we observe a similar phenomenon whereby the liver induces hepatokines in response to the chronic feeding of a lipid-rich diet. Whole body KO mice of Acadvl and a skeletal muscle-specific KO of Cpt1b are similarly resistant to HFD-induced sequelae (Vandanmagsar et al., 2016; Wicks et al., 2015; Zhang et al., 2010). Other models of impaired mitochondrial oxidative metabolism are also resistant to HFD-induced obesity and glucose intolerance, presumably via a hormetic response as well (Chung et al., 2017; Pospisilik et al., 2007). Similarly, part of the mechanism of action of the anti-diabetic drug metformin may be a mild inhibition of mitochondrial electron transport chain (Owen et al., 2000). The benefits of altered substrate utilization may be the generation of a stress response via an imbalance between substrate

flux and cellular demand rather than an elimination of excess nutrients per se. Defining the similarities between a gain and loss of hepatic substrate oxidation may identify the most effective biological interventions to treat the metabolic syndrome.

The failure to suppress hepatic glucose production is a hallmark of insulin resistance and type II diabetes. Although the transcriptional and hormonal control of gluconeogenesis in hepatocytes are important regulators of hepatic glucose metabolism, the systemic regulation and delivery of substrates for hepatic gluconeogenesis represents another important mode of regulation. That is, the availability of substrates to generate intramitochondrial acetyl-CoA and NADH is sufficient to drive inappropriate glucose production (Perry et al., 2015; Titov et al., 2016). Defects in hepatic lipid metabolism and oxidative stress have been implicated in the etiology of insulin resistance. Our data suggest that the inability of $Cpt2^{L-/-}$ mice to support hepatic gluconeogenesis is sufficient to protect mice from glucose intolerance following a HFD by lowering fasting blood glucose even though the rate of glucose disposal is similar. Consistent with this idea are mice with a hepatic-specific deletion in glucose-6-phosphatase, which are resistant to HFD-induced obesity and glucose intolerance (Abdul-Wahed et al., 2014; Mutel et al., 2011). Additionally, the improvement in glucose handling in $Cpt2^{L-/-}$ mice that exhibit high hepatic oxidative stress suggest that hepatic oxidative stress is not sufficient to drive glucose intolerance and supports the idea that inhibiting gluconeogenesis is an effective strategy to improve glucose levels in diabetes. Finally, $Cpt2^{L-/-}$ mice are extremely carnitine-deficient, similar to human inborn errors of fatty acid oxidation. The liver is one of the major organs responsible for synthesizing carnitine, and previous studies have shown that carnitine supplementation is beneficial for glucose tolerance (Noland et al., 2009; Power et al., 2007; Ringseis et al., 2012). It is not clear if carnitine administration to people with diabetes will ultimately prove successful; however, our results show that carnitine deficiency does not contribute to insulin resistance in our model.

One of the most surprising results from the current study is that $Cpt2^{L-/-}$ mice do not exhibit potentiated hepatic steatosis following chronic high-fat feeding. Fasting or a ketogenic diet greatly increases fatty liver in $Cpt2^{L-/-}$ mice (Lee et al., 2016b). However, $Cpt2^{L-/-}$ mice fed a chronic HFD did not exhibit potentiated liver TAG. Fasting imparts an immediate delivery of free fatty acids from adipose tissue to the liver. Adipose lipolysis generates fatty acids in excess of need, and surplus fatty acids are repackaged and exported in lipoproteins through the circulation. The difference between fasting and dietary lipids may simply be the kinetics as the slower yet continuous delivery of dietary lipids may be exported efficiently to non-hepatic tissues. Humans with fatty liver disease do not exhibit suppressed fatty acid oxidation but instead have enhanced hepatic fatty acid oxidation, although it is not clear if the rate is still insufficient for supply (Koliaki et al., 2015).

In conclusion, we have generated mice with a hepatocyte-specific deficiency of mitochondrial long chain fatty acid β-oxidation. These mice are paradoxically resistant to HFD-induced obesity and glucose intolerance in the absence of exacerbated liver disease. Although $Cpt2^{L-/-}$ mice have several hallmarks of diabetic liver, including increased hepatic oxidative stress and systemic carnitine deficiency, they are protected from glucose intolerance. The notion of increasing substrate oxidation in brown adipose tissue, skeletal

muscle or liver as a means of losing body weight may simply prove unrealistic in the face of complex systemic physiological adaptations (Lee et al., 2016a; Lee et al., 2015; Rodriguez et al., 2014; Vandanmagsar et al., 2016; Wicks et al., 2015). However, harnessing the systemic components responsible for hormesis may represent a path towards rational therapies for obese and diabetic patients.

## EXPERIMENTAL PROCEDURES

### Animals

Cpt2 $^{lox/lox}$ and Cpt2$^{L-/-}$ mice were previously described (Lee et al., 2016b). Mice were housed in ventilated racks with a 14hr-light/10hr-dark cycle and fed a standard chow diet (2018SX Teklad global). For diet studies, Cpt2 $^{lox/lox}$ and Cpt2$^{L-/-}$ mice were either fed a 60% high fat diet (D12492, Research Diets) or a low fat diet (D12450J, Research diets) starting at 6wks of age and continuing for 16wks. At the end of the diet study, fat and lean mass were measured via magnetic resonance imaging analysis (QNMR EchoMRI100; Echo Medical Systems). Analysis of metabolites were done for free glycerol and TAG (Sigma), β-hydroxybutyrate (StanBio), total cholesterol, NEFA (Wako), Bile acids (BioVision), TBARS and Glutathione (Cayman) and ALT activity (Sigma). Serum insulin (Crystal Chem), Fgf21, Gdf15, Igfbp1 and Adiponectin (R&D Systems) were measured by ELISA. Total saponified fatty acids were quantified by GCMS as we have previously described (Bowman et al., 2017; Reamy and Wolfgang, 2011). Acylcarnitines were quantified as previously described (Lee et al., 2016b). Urine acylcarnitine levels were normalized to creatinine levels in urine (Cayman). Glucose and insulin tolerance tests were performed as described (Lee et al., 2015). To determine whole body bioenergetics, mice were fed a 60% HFD at 9 weeks of age and continued for 4 weeks prior to the experiment. At 13 weeks of age, body fat and lean mass of Cpt2 $^{lox/lox}$ and Cpt2$^{L-/-}$ mice were determined via magnetic resonance imaging. Then these mice were then individually housed in Oxymax indirect calorimetry cages (Columbus Instruments). Indirect calorimetry and metabolic cage studies were normalized to lean mass as described (Ellis et al., 2013). Hyperinsulinemic-Euglycemic studies were performed as described (Kim, 2009). All procedures were performed in accordance with the NIH's Guide for the Car and Use of Laboratory Animals and under the approval of the Johns Hopkins Medical School Animal Care and Use Committee.

### NMR Spectroscopy

Steady-state $^{1}$H NMR Spectroscopy was done as previously described(Gonzalez-Hurtado et al., 2017; Selen et al., 2015). $^{13}$C NMR spectra were collected using a zgpg30 pulse program on a 500MHz Bruker Avance III (Bruker, Germany). Each sample was tuned, matched and shimmed using TopShim before the acquisition of the spectrum. 65536 data points were collected with spectra width of 29762 Hz. 16000 scans were collected for each $^{13}$C spectrum, with acquisition time of 1.1sec and a relaxation delay of 1.5 sec. Proton decoupling was performed using a standard WALTZ16 pulse sequence. Mestrenova was used to analyze $^{13}$C and 2D HSQC spectra. $^{1}$D $^{13}$C spectra were zero filled to 128K data points. 0.1mM dioxane was used as internal reference and the chemical shift was calibrated by referencing dioxane signal to 67.4 ppm. $^{1}$D $^{13}$C spectra were manually phase corrected and spline function was applied for the baseline correction (Mestrenova, Spain). The peak

height of dioxane was used to normalize the peak height of the carbon signals of glucose. BMRB $^{13}C$ glucose reference spectrum (500MHz, Bruker Avance) was used to profile the glucose peaks in the spectra. 2D 1H, 13C- heteronuclear single quantum coherence spectroscopy (HSQC) NMR spectra were acquired using 500MHz Bruker Avance. 2D data collected with 16 scans using Bruker pulse program 'hsqcetgp' 2D 1H, $^{13}C$-HSQC spectra were used for further verification of the peaks of interest in $^{13}C$ spectra.

### Steady-State Metabolite Analysis with HPLC-QTOF

Frozen 50–100mg Cpt2 $^{lox/lox}$ and Cpt2$^{L-/-}$ liver tissue were homogenized in 600ul ice-cold methanol and centrifuged at 12,000rpm for 15 minutes. Supernatant was transferred to a new tube and the pellet was extracted with methanol-water (80%–20%) followed by a second centrifuge. Supernatants were combined and left in a speed-vac for overnight drying. Pellet was used for protein quantification. Dried materials were reconstituted in 200ul acetonitrile-water (80%–20%). Chromatographic separation (HPLC) was performed with Supelco Discovery HS F5-3 column (15cm*2.1mm, 3um). The HPLC system (Agilent 1200 series) was operated at the flow rate 0.5 mL/min with solvent A (water with 0.1% formic acid), and solvent B (acetonitrile). The LC parameters were set as follows; auto sampler temperature 4C and injection volume 4ul. Gradient conditions were; 0–15min; 100% A, 15–18 min; 70% A, 19–26 min; 50% A, 27–35min; 0% A, 35.10–50 min; 100% A. Metabolomics experiment was performed on an Agilent QTOF LC/MS system (Agilent Tech 6520). Data were collected in negative mode. Data analysis performed using Agilent Profinder Software.

### Real time PCR

RNA was isolated from all tissues using the RNeasy Mini Kit (QIAGEN). Using the High Capacity cDNA Reverse Transcription Kit (Applied Biosystems), we reverse transcribed 1–2μg of total RNA. The cDNA was diluted to 2 ng/μl and amplified by primers in a 20-μl reaction using SsoAdvanced SYBR Green Supermix (BioRad). We calculated mRNA using a 2^deltaCT relative to the average of the housekeeping genes *cyclophilinA* and *rpl22* expression. All primers and gene information were previously reported (Lee et al., 2015) or provided in Table S1.

### Western blots

Liver homogenates from 16-week HFD or acute insulin injected Cpt2 $^{lox/lox}$ and Cpt2$^{L-/-}$ mice were prepared using 1x RIPA buffer with protease and phosphatase inhibitors. The protein concentration was measured using the Pierce BCA Protein Assay kit (Thermo Scientific). We used 30μg of protein on an SDS-PAGE and then transferred it to a nitrocellulose (Protran BA 83, Whatman) membrane. We then blocked with 3% BSA-TBST (Tris-buffered saline with Tween20). The membranes were probed with antibodies Pcx (Cell Signaling), Acly (Cell Signaling), Total Acc (Cell Signaling), Fasn (BD Biosciences), Scd1 (Cell Signaling), Hsp27 (Cell Signaling), Mitoprofile (Abcam) and Hsc70 (Santa Cruz Biotechnology) diluted 1:1000 with 3% BSA in TBST. Hsc70 used the appropriate Cy3 fluorescent secondary antibody, and the other primary antibodies used corresponding secondary antibodies conjugated to horseradish peroxidase. Images were collected using an Alpha Innotech FluorChemQ and presented with minimal image processing.

### Statistical analysis

Data were analyzed with the assistance of Prism. Significance was determined using an unpaired two-tailed t test for single variable experiments and two-way ANOVA with Bonferroni post hoc correction for multiple variable experiments.

## Supplementary Material

Refer to Web version on PubMed Central for supplementary material.

## Acknowledgments

We would like to thank Natasha Zachara for essential reagents, Susan Aja for metabolic cage studies and Caitlyn Bowman for helpful discussion. We would like to thank Ann Moser at the Kennedy Krieger Institute for assistance in GC/MS analysis of fatty acids. This work was supported in part by a National Institutes of Health grant R01NS072241 and American Diabetes Association grant #1-16-IBS-313 to M.J.W. The bone phenotyping was performed at the Baltimore Diabetes Research Center and funded by NIH grant DK079637. Part of this study was performed at the National Mouse Metabolic Phenotyping Center at UMass Medical School and funded by NIH grant U2C-DK093000.

## References

Abdul-Wahed A, Gautier-Stein A, Casteras S, Soty M, Roussel D, Romestaing C, Guillou H, Tourette JA, Pleche N, Zitoun C, et al. A link between hepatic glucose production and peripheral energy metabolism via hepatokines. Mol Metab. 2014; 3:531–543. [PubMed: 25061558]

An J, Muoio DM, Shiota M, Fujimoto Y, Cline GW, Shulman GI, Koves TR, Stevens R, Millington D, Newgard CB. Hepatic expression of malonyl-CoA decarboxylase reverses muscle, liver and whole-animal insulin resistance. Nature medicine. 2004; 10:268–274.

Bowman CE, Rodriguez S, Selen Alpergin ES, Acoba MG, Zhao L, Hartung T, Claypool SM, Watkins PA, Wolfgang MJ. The Mammalian Malonyl-CoA Synthetase ACSF3 Is Required for Mitochondrial Protein Malonylation and Metabolic Efficiency. Cell Chem Biol. 2017

Chen X, Iqbal N, Boden G. The effects of free fatty acids on gluconeogenesis and glycogenolysis in normal subjects. J Clin Invest. 1999; 103:365–372. [PubMed: 9927497]

Chung HK, Ryu D, Kim KS, Chang JY, Kim YK, Yi HS, Kang SG, Choi MJ, Lee SE, Jung SB, et al. Growth differentiation factor 15 is a myomitokine governing systemic energy homeostasis. The Journal of cell biology. 2017; 216:149–165. [PubMed: 27986797]

Ellis JM, Wong GW, Wolfgang MJ. Acyl coenzyme A thioesterase 7 regulates neuronal fatty acid metabolism to prevent neurotoxicity. Mol Cell Biol. 2013; 33:1869–1882. [PubMed: 23459938]

Gonzalez-Hurtado E, Lee J, Choi J, Selen Alpergin ES, Collins SL, Horton MR, Wolfgang MJ. The Loss Of Macrophage Fatty Acid Oxidation Does Not Potentiate Systemic Metabolic Dysfunction. Am J Physiol Endocrinol Metab. 2017 ajpendo 00408 02016.

Kerner J, Hoppel C. Fatty acid import into mitochondria. Biochim Biophys Acta. 2000; 1486:1–17. [PubMed: 10856709]

Kim JK. Hyperinsulinemic-euglycemic clamp to assess insulin sensitivity in vivo. Methods in molecular biology (Clifton, NJ. 2009; 560:221–238.

Koliaki C, Szendroedi J, Kaul K, Jelenik T, Nowotny P, Jankowiak F, Herder C, Carstensen M, Krausch M, Knoefel WT, et al. Adaptation of hepatic mitochondrial function in humans with non-alcoholic fatty liver is lost in steatohepatitis. Cell Metab. 2015; 21:739–746. [PubMed: 25955209]

Lee J, Choi J, Aja S, Scafidi S, Wolfgang MJ. Loss of Adipose Fatty Acid Oxidation Does Not Potentiate Obesity at Thermoneutrality. Cell Rep. 2016a; 14:1308–1316. [PubMed: 26854223]

Lee J, Choi J, Scafidi S, Wolfgang MJ. Hepatic Fatty Acid Oxidation Restrains Systemic Catabolism during Starvation. Cell Rep. 2016b; 16:201–212. [PubMed: 27320917]

Lee J, Ellis JM, Wolfgang MJ. Adipose fatty acid oxidation is required for thermogenesis and potentiates oxidative stress-induced inflammation. Cell Rep. 2015; 10:266–279. [PubMed: 25578732]

Lee JM, Wagner M, Xiao R, Kim KH, Feng D, Lazar MA, Moore DD. Nutrient-sensing nuclear receptors coordinate autophagy. Nature. 2014; 516:112–115. [PubMed: 25383539]

Mashek DG. Hepatic fatty acid trafficking: multiple forks in the road. Adv Nutr. 2013; 4:697–710. [PubMed: 24228201]

McGarry JD, Brown NF. The mitochondrial carnitine palmitoyltransferase system. From concept to molecular analysis. Eur J Biochem. 1997; 244:1–14. [PubMed: 9063439]

Mutel E, Gautier-Stein A, Abdul-Wahed A, Amigo-Correig M, Zitoun C, Stefanutti A, Houberdon I, Tourette JA, Mithieux G, Rajas F. Control of blood glucose in the absence of hepatic glucose production during prolonged fasting in mice: induction of renal and intestinal gluconeogenesis by glucagon. Diabetes. 2011; 60:3121–3131. [PubMed: 22013018]

Noland RC, Koves TR, Seiler SE, Lum H, Lust RM, Ilkayeva O, Stevens RD, Hegardt FG, Muoio DM. Carnitine insufficiency caused by aging and overnutrition compromises mitochondrial performance and metabolic control. The Journal of biological chemistry. 2009; 284:22840–22852. [PubMed: 19553674]

Orellana-Gavalda JM, Herrero L, Malandrino MI, Paneda A, Sol Rodriguez-Pena M, Petry H, Asins G, Van Deventer S, Hegardt FG, Serra D. Molecular therapy for obesity and diabetes based on a long-term increase in hepatic fatty-acid oxidation. Hepatology. 2011; 53:821–832. [PubMed: 21319201]

Owen MR, Doran E, Halestrap AP. Evidence that metformin exerts its anti-diabetic effects through inhibition of complex 1 of the mitochondrial respiratory chain. Biochem J. 2000; 348(Pt 3):607–614. [PubMed: 10839993]

Perry RJ, Camporez JP, Kursawe R, Titchenell PM, Zhang D, Perry CJ, Jurczak MJ, Abudukadier A, Han MS, Zhang XM, et al. Hepatic acetyl CoA links adipose tissue inflammation to hepatic insulin resistance and type 2 diabetes. Cell. 2015; 160:745–758. [PubMed: 25662011]

Perry RJ, Kim T, Zhang XM, Lee HY, Pesta D, Popov VB, Zhang D, Rahimi Y, Jurczak MJ, Cline GW, et al. Reversal of hypertriglyceridemia, fatty liver disease, and insulin resistance by a liver-targeted mitochondrial uncoupler. Cell metabolism. 2013; 18:740–748. [PubMed: 24206666]

Pospisilik JA, Knauf C, Joza N, Benit P, Orthofer M, Cani PD, Ebersberger I, Nakashima T, Sarao R, Neely G, et al. Targeted deletion of AIF decreases mitochondrial oxidative phosphorylation and protects from obesity and diabetes. Cell. 2007; 131:476–491. [PubMed: 17981116]

Potthoff MJ, Kliewer SA, Mangelsdorf DJ. Endocrine fibroblast growth factors 15/19 and 21: from feast to famine. Genes Dev. 2012; 26:312–324. [PubMed: 22302876]

Power RA, Hulver MW, Zhang JY, Dubois J, Marchand RM, Ilkayeva O, Muoio DM, Mynatt RL. Carnitine revisited: potential use as adjunctive treatment in diabetes. Diabetologia. 2007; 50:824–832. [PubMed: 17310372]

Reamy AA, Wolfgang MJ. Carnitine palmitoyltransferase-1c gain-of-function in the brain results in postnatal microencephaly. Journal of neurochemistry. 2011; 118:388–398. [PubMed: 21592121]

Ringseis R, Keller J, Eder K. Role of carnitine in the regulation of glucose homeostasis and insulin sensitivity: evidence from in vivo and in vitro studies with carnitine supplementation and carnitine deficiency. Eur J Nutr. 2012; 51:1–18. [PubMed: 22134503]

Rodriguez S, Ellis JM, Wolfgang MJ. Chemical-genetic induction of Malonyl-CoA decarboxylase in skeletal muscle. BMC Biochem. 2014; 15:20. [PubMed: 25152047]

Samuel VT, Liu ZX, Qu X, Elder BD, Bilz S, Befroy D, Romanelli AJ, Shulman GI. Mechanism of hepatic insulin resistance in non-alcoholic fatty liver disease. J Biol Chem. 2004; 279:32345–32353. [PubMed: 15166226]

Savage DB, Petersen KF, Shulman GI. Disordered lipid metabolism and the pathogenesis of insulin resistance. Physiol Rev. 2007; 87:507–520. [PubMed: 17429039]

Selen ES, Bolandnazar Z, Tonelli M, Butz DE, Haviland JA, Porter WP, Assadi-Porter FM. NMR Metabolomics Show Evidence for Mitochondrial Oxidative Stress in a Mouse Model of Polycystic Ovary Syndrome. J Proteome Res. 2015; 14:3284–3291. [PubMed: 26076986]

Soling HD, Willms B, Friedrichs D, Kleineke J. Regulation of gluconeogenesis by fatty acid oxidation in isolated perfused livers of non-starved rats. Eur J Biochem. 1968; 4:364–372. [PubMed: 5653769]

Stefanovic-Racic M, Perdomo G, Mantell BS, Sipula IJ, Brown NF, O'Doherty RM. A moderate increase in carnitine palmitoyltransferase 1a activity is sufficient to substantially reduce hepatic triglyceride levels. Am J Physiol Endocrinol Metab. 2008; 294:E969–977. [PubMed: 18349115]

Szendroedi J, Phielix E, Roden M. The role of mitochondria in insulin resistance and type 2 diabetes mellitus. Nat Rev Endocrinol. 2011; 8:92–103. [PubMed: 21912398]

Titov DV, Cracan V, Goodman RP, Peng J, Grabarek Z, Mootha VK. Complementation of mitochondrial electron transport chain by manipulation of the NAD+/NADH ratio. Science. 2016; 352:231–235. [PubMed: 27124460]

Vandanmagsar B, Warfel JD, Wicks SE, Ghosh S, Salbaum JM, Burk D, Dubuisson OS, Mendoza TM, Zhang J, Noland RC, et al. Impaired Mitochondrial Fat Oxidation Induces FGF21 in Muscle. Cell Rep. 2016; 15:1686–1699. [PubMed: 27184848]

Wang X, Wei W, Krzeszinski JY, Wang Y, Wan Y. A Liver-Bone Endocrine Relay by IGFBP1 Promotes Osteoclastogenesis and Mediates FGF21-Induced Bone Resorption. Cell Metab. 2015; 22:811–824. [PubMed: 26456333]

Wicks SE, Vandanmagsar B, Haynie KR, Fuller SE, Warfel JD, Stephens JM, Wang M, Han X, Zhang J, Noland RC, et al. Impaired mitochondrial fat oxidation induces adaptive remodeling of muscle metabolism. Proceedings of the National Academy of Sciences of the United States of America. 2015; 112:E3300–3309. [PubMed: 26056297]

Wolfe, RR. Radioactive and Stable Isotope Tracers in Biomedicine: Principles and Practice of Kinetic Analysis. Wiley; 1992.

Yun J, Finkel T. Mitohormesis. Cell Metab. 2014; 19:757–766. [PubMed: 24561260]

Zhang D, Christianson J, Liu ZX, Tian L, Choi CS, Neschen S, Dong J, Wood PA, Shulman GI. Resistance to high-fat diet-induced obesity and insulin resistance in mice with very long-chain acyl-CoA dehydrogenase deficiency. Cell Metab. 2010; 11:402–411. [PubMed: 20444420]

Zhang D, Liu ZX, Choi CS, Tian L, Kibbey R, Dong J, Cline GW, Wood PA, Shulman GI. Mitochondrial dysfunction due to long-chain Acyl-CoA dehydrogenase deficiency causes hepatic steatosis and hepatic insulin resistance. Proceedings of the National Academy of Sciences of the United States of America. 2007; 104:17075–17080. [PubMed: 17940018]

## Highlights

- Loss of hepatic fatty acid oxidation (FAO) confers resistance to obesity.
- Loss of hepatic FAO results in beneficial hormesis.
- The suppression of FAO is sufficient to improve diet-induced glucose intolerance.
- Resistance to obesity results from increased energy expenditure.

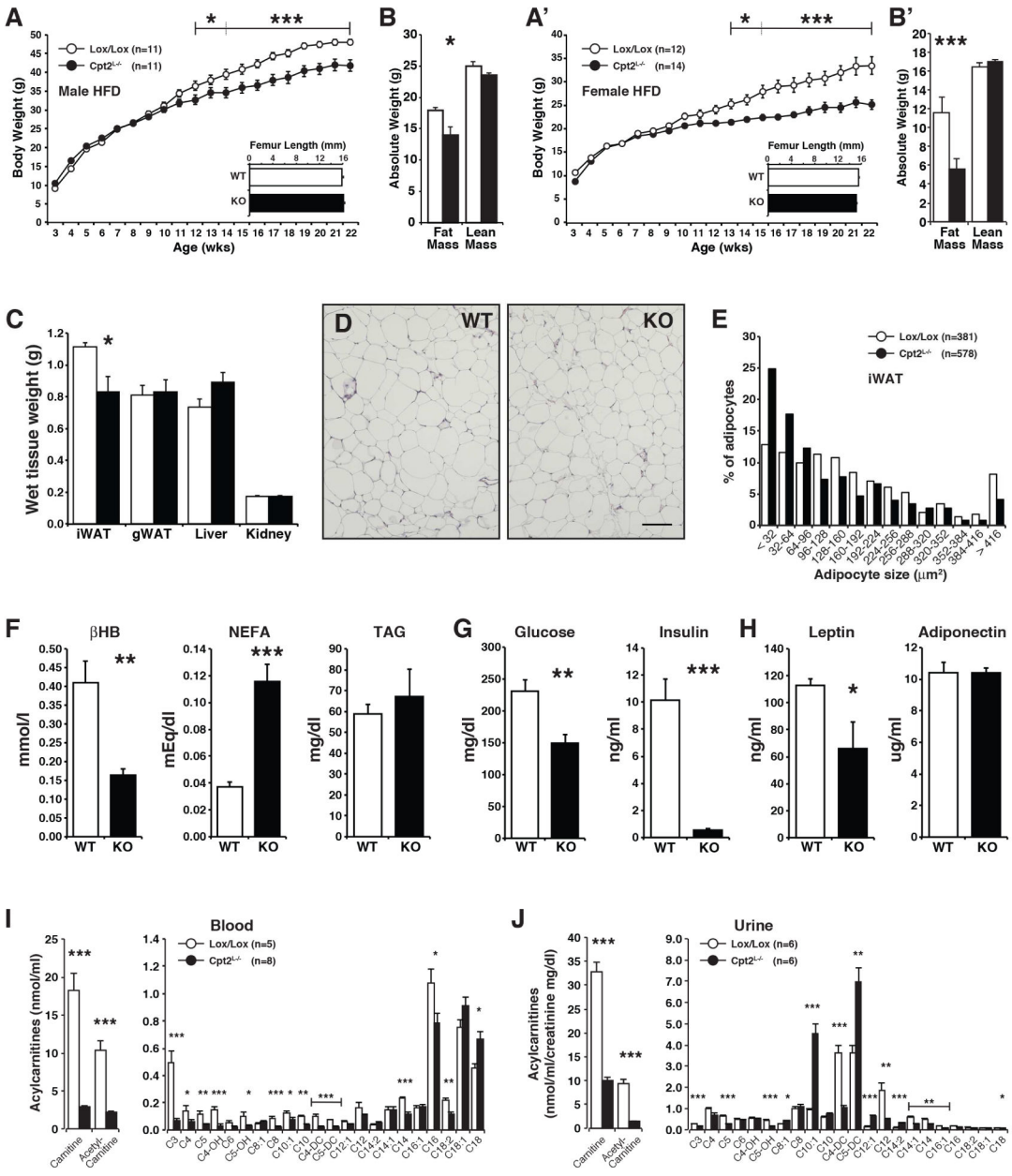


**Figure 1. Liver-specific deficiency in fatty acid oxidation is protective against HFD-induced body weight gain and adiposity**

(A) Body weight and femur lengths of male Cpt2$^{lox/lox}$ and Cpt2$^{L-/-}$ mice fed a HFD for 16wks (n=12).

(B) Body compositions of male Cpt2$^{lox/lox}$ and Cpt2$^{L-/-}$ mice fed a HFD for 16wks measured by EchoMRI (n=12).

(C) Wet weights of iWAT and gWAT unilateral depots, liver (left lobe) and kidney for male Cpt2$^{lox/lox}$ and Cpt2$^{L-/-}$ mice fed a HFD for 16wks (n=12).

(D) H&E stained sections of iWAT from male Cpt2$^{lox/lox}$ and Cpt2$^{L-/-}$ mice fed a HFD for 16wks. Scale bar, 100 μm.

(E) Adipocyte size distribution from H&E stained sections of iWAT from $Cpt2^{lox/lox}$ and $Cpt2^{L-/-}$ mice fed a HFD for 16wks.
(F) Serum metabolites in male $Cpt2^{lox/lox}$ and $Cpt2^{L-/-}$ mice fed a HFD for 16wks (n=6).
(G) Serum lucose and insulin in male $Cpt2^{lox/lox}$ and $Cpt2^{L-/-}$ mice fed a HFD for 16wks (n=6).
(H) Serum leptin and adiponectin in male $Cpt2^{lox/lox}$ and $Cpt2^{L-/-}$ mice fed a HFD for 16wks (n=6).
(I) Blood acylcarnitines of male $Cpt2^{lox/lox}$ and $Cpt2^{L-/-}$ mice following a 16-week chronic high fat feeding (n=5–8).
(J) Urine acylcarnitines of male $Cpt2^{lox/lox}$ and $Cpt2^{L-/-}$ mice following a 16-week chronic high fat feeding (n=6). Urine acylcarnitine values were normalized to creatinine values.
Data are expressed as mean ± SEM. *p<0.05; **p<0.01; ***p<0.001.

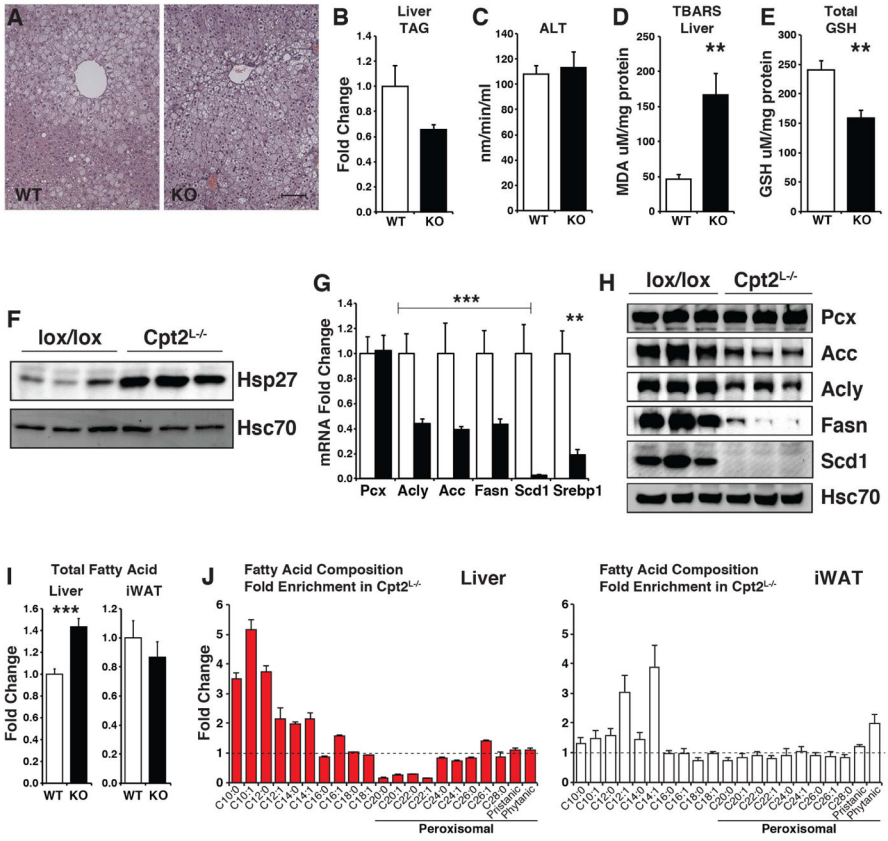


**Figure 2. Loss of hepatic fatty acid oxidation induces oxidative stress**

(A) H&E stained sections of liver from male Cpt2$^{lox/lox}$ and Cpt2$^{L-/-}$ mice fed a HFD for 16wks.

(B) Liver TAG content of male Cpt2$^{lox/lox}$ and Cpt2$^{L-/-}$ mice fed a HFD for 16wks (n=6).

(C) Measure of liver damage via serum ALT activity in male Cpt2$^{lox/lox}$ and Cpt2$^{L-/-}$ mice fed a HFD for 16wks (n=6).

(D) TBARS assay measuring lipid peroxidation in liver of male Cpt2$^{lox/lox}$ and Cpt2$^{L-/-}$ mice fed a HFD for 16wks (n=6).

(E) Total glutathione in livers of Cpt2$^{lox/lox}$ and Cpt2$^{L-/-}$ mice fed a HFD for 16wks (n=7).

(F) Western blot of Hsp27 in livers of Cpt2$^{lox/lox}$ and Cpt2$^{L-/-}$ mice fed a HFD for 16wks.

(G) Gene expression of fatty acid synthesis genes in livers of Cpt2$^{lox/lox}$ and Cpt2$^{L-/-}$ mice fed a HFD for 16wks (n=6).

(H) Western blots of proteins in fatty acid synthesis in livers of Cpt2$^{lox/lox}$ and Cpt2$^{L-/-}$ mice fed a HFD for 16wks. All blots were normalized to Hsc70.

(I) Total saponified fatty acid concentration in Liver and iWAT of Cpt2$^{lox/lox}$ and Cpt2$^{L-/-}$ mice fed a HFD for 16wks (n=5–6). See also Table S2.

(J) Enrichment of fatty acids by chain length in Liver and iWAT of Cpt2$^{lox/lox}$ and Cpt2$^{L-/-}$ mice fed a HFD for 16wks (n=5–6). See also Table S2.

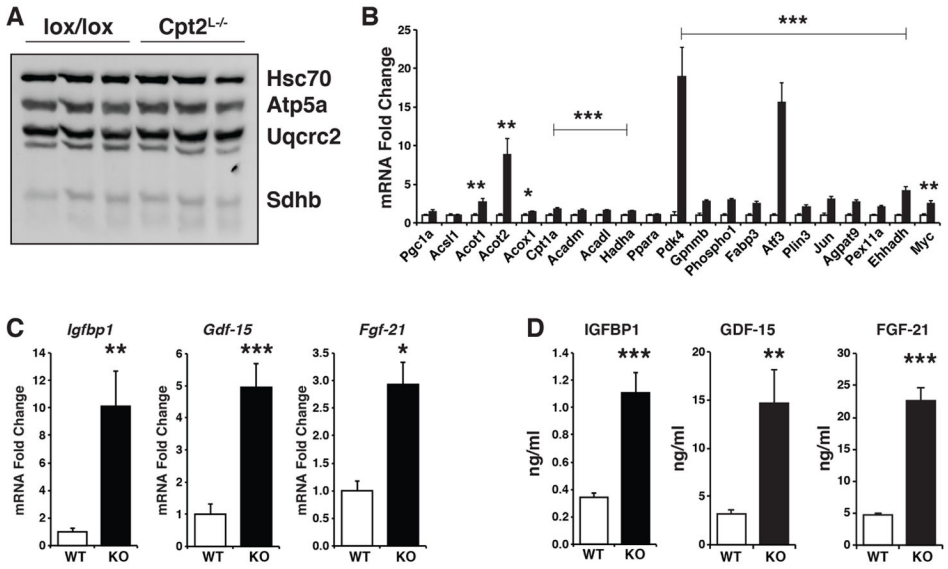


**Figure 3. Loss of hepatic fatty acid oxidation induces hepatokines**

(A) Western blot for mitochondrial complexes and Hsc70 in livers of $Cpt2^{lox/lox}$ and $Cpt2^{L-/-}$ mice fed a HFD for 16wks.

(B) Gene expression of fatty acid metabolism and Pparα target genes in livers of $Cpt2^{lox/lox}$ and $Cpt2^{L-/-}$ mice fed a HFD for 16wks (n=6).

(C) Liver mRNA of *igfbp1*, *gdf15*, and *fgf21* in $Cpt2^{lox/lox}$ and $Cpt2^{L-/-}$ mice fed a HFD for 16wks (n=6).

(D) Serum concentrations of Igfbp1, Gdf15 and Fgf21 in $Cpt2^{lox/lox}$ and $Cpt2^{L-/-}$ mice fed a HFD for 16wks (n=6).

Data are expressed as mean ± SEM. *p<0.05; **p<0.01; ***p<0.001.

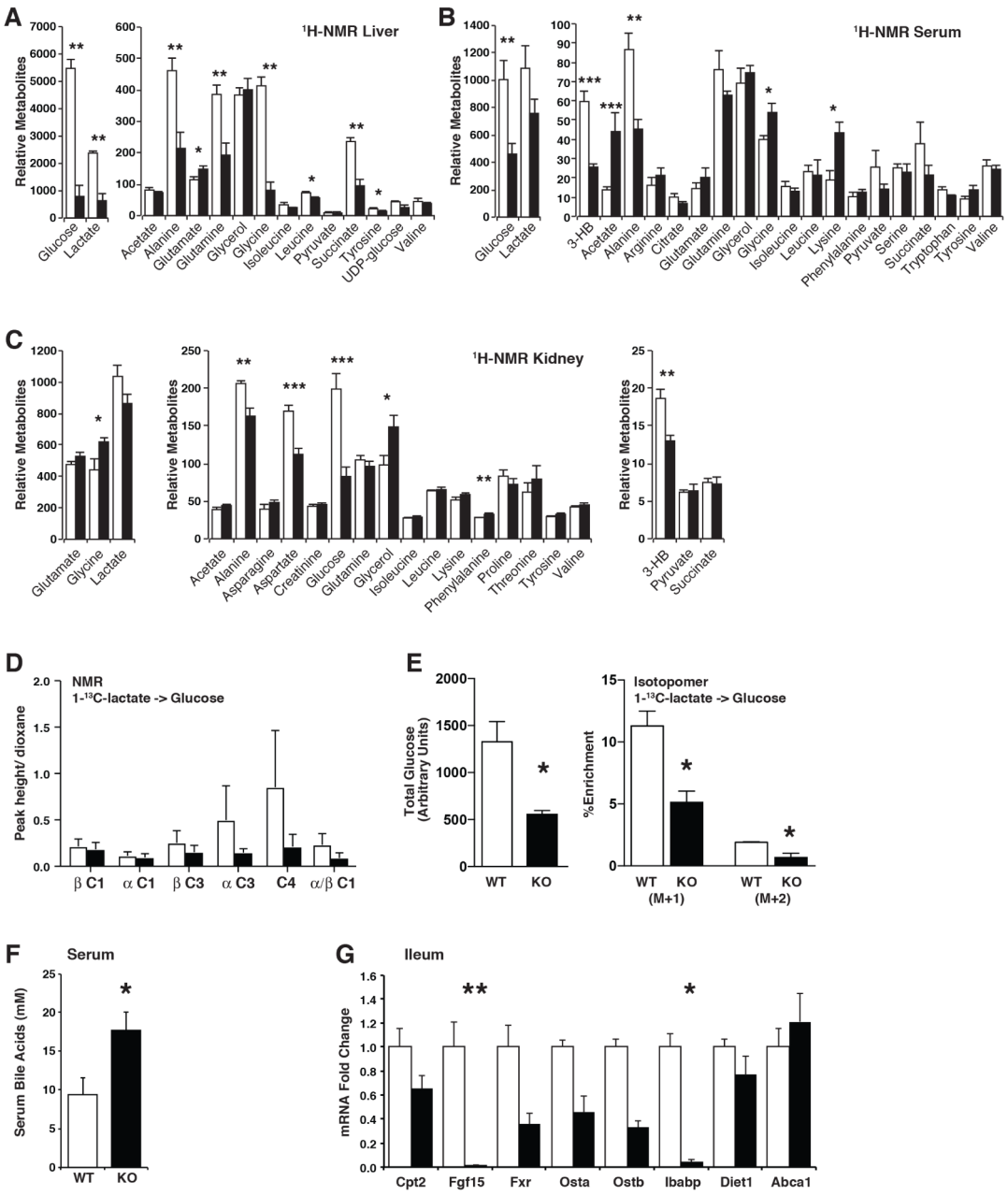


**Figure 4. Metabolic alterations upon the loss of hepatic fatty acid oxidation**

(E) $^{1}$H-NMR in liver of Cpt2$^{lox/lox}$ and Cpt2$^{L-/-}$ mice fed a high fat diet for 16 weeks (n=6).

(F) $^{1}$H-NMR in serum of Cpt2$^{lox/lox}$ and Cpt2$^{L-/-}$ mice fed a high fat diet for 16 weeks (n=6).

(G) $^{1}$H-NMR in kidney of Cpt2$^{lox/lox}$ and Cpt2$^{L-/-}$ mice fed a high fat diet for 16 weeks (n=6).

(H) NMR analysis of 1-$^{13}$C-lactate incorporation into glucose in 24hr fasted mice (n=3).

(I) Isotopomer analysis of 1-$^{13}$C-lactate incorporation into glucose in 24hr fasted mice (n=3).

(J) Total bile acids in serum of Cpt2$^{lox/lox}$ and Cpt2$^{L-/-}$ mice fed a HFD for 9wks (n=4–7).

(K) Bile acid metabolic genes in ileum of $Cpt2^{lox/lox}$ and $Cpt2^{L-/-}$ mice fed a HFD for 9wks (n=4).

Data are expressed as mean ± SEM. *p<0.05; **p<0.01; ***p<0.001.

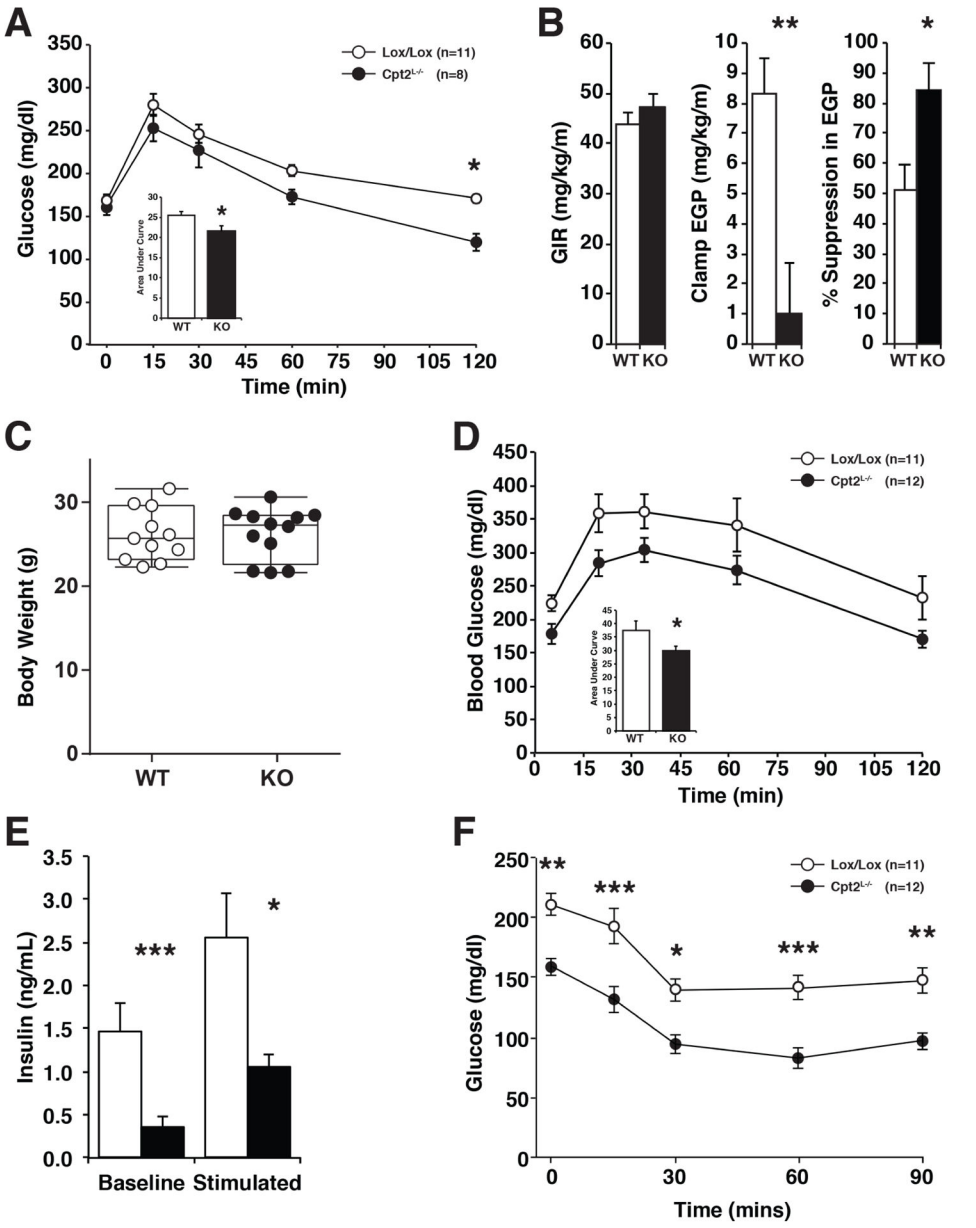


**Figure 5. Loss of hepatic fatty acid oxidation improves glucose tolerance and insulin sensitivity**

(A) Intraperitoneal glucose tolerance test (ipGTT) including area under the curve in male $Cpt2^{lox/lox}$ and $Cpt2^{L-/-}$ mice fed a chow diet (n=8–11).

(B) Hyperinsulinemic-euglycemic clamp showing glucose infusion rate (GIR), endogenous glucose production (EGP) and insulin suppression of EGP (n=7–9).

(C) Body weight of male $Cpt2^{lox/lox}$ and $Cpt2^{L-/-}$ mice fed a high fat diet for 4 wks (n=11–12).

(D) ipGTT including area under the curve in male $Cpt2^{lox/lox}$ and $Cpt2^{L-/-}$ mice fed a high fat diet for 4 wks (n=11–12).

(E) Serum insulin levels measured at baseline and glucose stimulated (15min) conditions in $Cpt2^{lox/lox}$ and $Cpt2^{L-/-}$ mice fed a high fat diet for 4 wks (n=6).

(F) Intraperitoneal insulin tolerance test (ipITT) including area above curve in male $Cpt2^{lox/lox}$ and $Cpt2^{L-/-}$ mice fed a high fat diet for 5 wks (n=11–12).
Data are expressed as mean ± SEM. *p<0.05; **p<0.01; ***p<0.001.

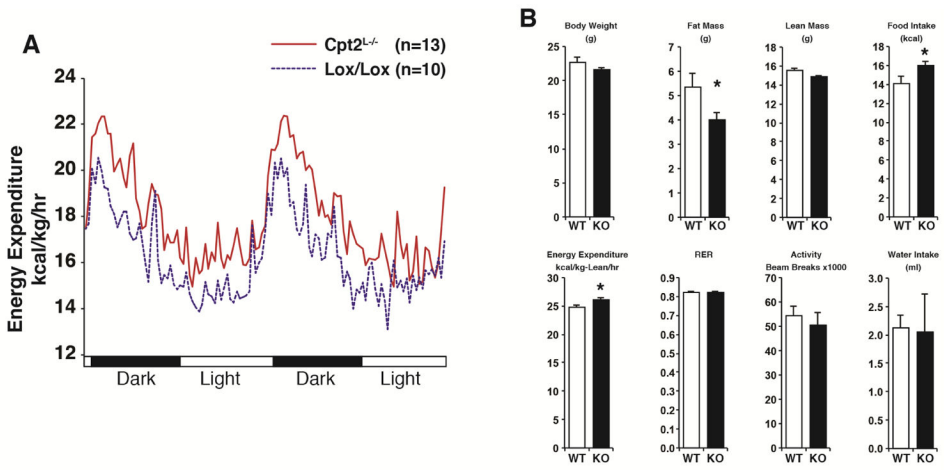


**Figure 6. Loss of hepatic fatty acid oxidation increases energy expenditure in response to high fat feeding**

(A) Energy expenditure under dark and light cycles of female Cpt2$^{lox/lox}$ and Cpt2$^{L-/-}$ mice after 4 wks on high fat diet (n=10–13).

(B) Metabolic parameters of female Cpt2$^{lox/lox}$ and Cpt2$^{L-/-}$ mice fed a HFD for 4wks (n=10–13).

Data are expressed as mean ± SEM. *p<0.05; **p<0.01; ***p<0.001.

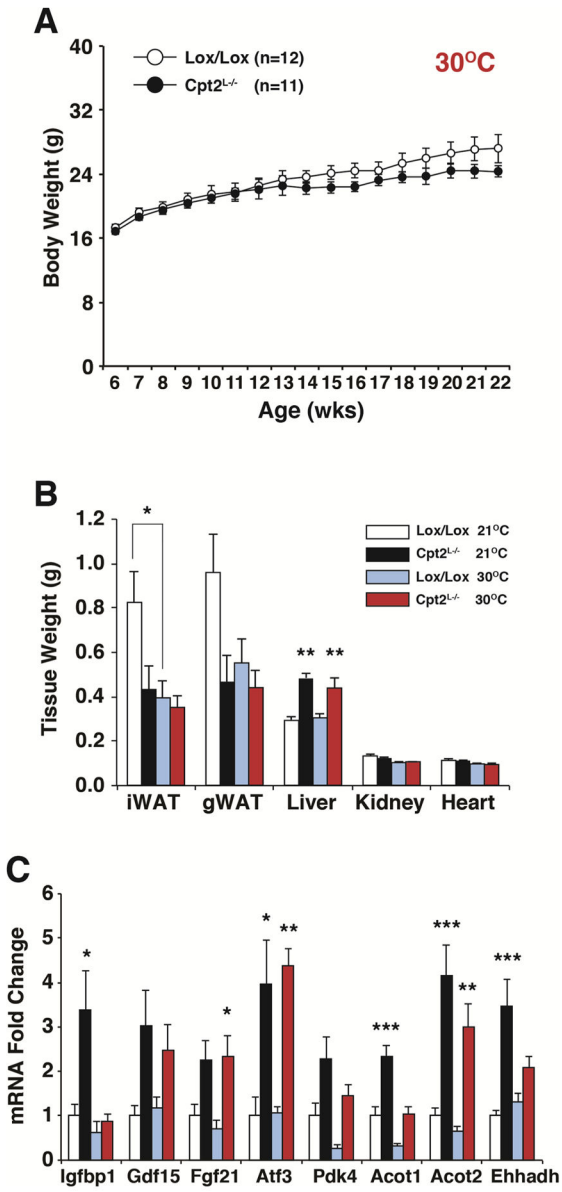


**Figure 7. Loss of hepatic fatty acid oxidation at thermoneutrality normalizes body weight during high fat feeding**

(A) Body weight of female Cpt2$^{lox/lox}$ and Cpt2$^{L-/-}$ mice fed a high fat diet at thermoneutrality (30°C) for 16 weeks (n=11–12).

(B) Wet weights of iWAT and gWAT unilateral depots, liver (left lobe), kidney and heart of female Cpt2$^{lox/lox}$ and Cpt2$^{L-/-}$ mice fed a HFD for 16wks at 21°C (n=12–14) or 30°C (n=11–12).

(C) Gene expression in livers of female Cpt2$^{lox/lox}$ and Cpt2$^{L-/-}$ mice fed a HFD for 16wks at 21°C or 30°C (n=6).

Data are expressed as mean ± SEM. *p<0.05; **p<0.01; ***p<0.001.